Numerical form-finding of geotensoid tension truss for mesh reflector

Sebastien Morterolle, Bernard Maurin, Jérôme Quirant, Christian Dupuy

Numerical form-finding of geotensoid tension truss for mesh reflector

Sébastien MORTEROLLE[1], Bernard MAURIN[1], Jérôme QUIRANT[1], Christian DUPUY[2]

[1] Laboratoire de Mécanique et Génie Civil, Université Montpellier 2, CC48, place E. Bataillon, 34095 Montpellier cedex 5, France.
[2] Centre National d'Etudes Spatiales, 18 avenue E. Belin, 31401Toulouse cedex 9, France.

Corresponding author: B. MAURIN, Laboratoire de Mécanique et Génie Civil, Université Montpellier 2, CC48, Place E. Bataillon, 34095 Montpellier cedex 5, France
bernard.maurin@univ-montp2.fr ; Tel: +33 4 67 14 46 80 ; Fax: +33 4 67 14 45 55

Abstract: The parabolic surface of most large deployable reflectors is formed by a reflective mesh attached to a cable net. This paper presents a new approach to calculate a geodesic tension truss that ensures both appropriate node positioning and uniform tension. It is based on a force density strategy coupled with geometrical constraints. Uniform tension is achieved by iterations on coefficients of force density. Nodes of net are located on the paraboloid by controlling additional forces. Several applications illustrate the method on various types of net patterns and parabolic surfaces. The accuracy of obtained net is then evaluated by calculation of the systematic surface error due to faceting. Attachment of the net to a rim structure with additional cables is also discussed.

Keywords: cable net, uniform tension, force density method

1. Introduction

Mesh reflectors are widely used for large aperture space antenna systems because they are lightweight, and can be packaged compactly and easily. Their radio-frequency surface consists of facetted reflective mesh. It is knitted from interlaced electrically conductive thin wires, made of gold-plated molybdenum, typically of 0.03 mm diameter. This mesh is stretched over a cable net, usually made of stiff unidirectional composite filaments, attached to a framework. The reflective surface is thus composed only of flexible elements and can be easily folded. Its accuracy however depends on the shape of the cable net.
Two main conceptual designs may be identified. The first one is based on a division of the parabolic surface in gores supported by radial ribs or radial cables attached to an outside ring (umbrella-type reflectors). The second strategy considers a division of the surface in flat facets formed by the cable net and tensioned with out-of-plane forces applied at every junction node (Figure 1). This tension truss concept was developed by Miura [1].

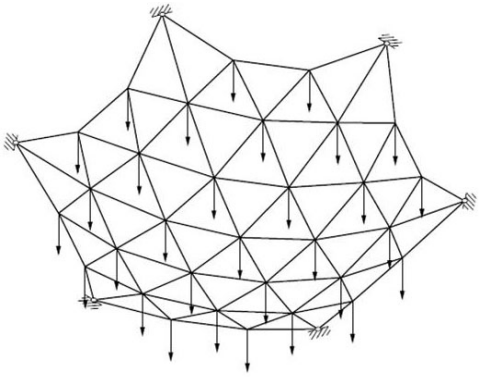

Figure 1: Tension truss formed by out-of-plane loads (from Tibert [2])

Several large deployable antennas using the tension truss concept have been tested and launched, such as the space radio telescope Halca or the AstroMesh reflector (Figure 2). It has also been studied by Tibert [3] to design an antenna based on a tensegrity structure.

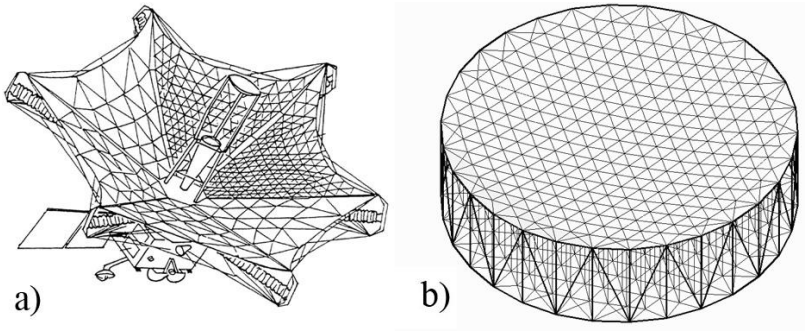

Figure 2: Tension truss antennas: a) Halca; b) AstroMesh

A fairly isotropic and uniform tension in the reflective mesh ensures good electrical conductivity and hence RF reflectivity. The mesh tension must be sufficient to withstand lateral accelerations greater than those experienced in orbit without severe distortion of the reflector surface. Mesh tensions from 5 to 10 N/m have been used in previous studies [4,5]; even if higher tension will more effectively smooth out the creases of mesh due to folding and thereby give better antenna performance. Uniform tension in the supporting cable net is moreover interesting from a geometrical and mechanical point of view. A cable with a constant tension positioned on a curved surface indeed follows its geodesic lines, resulting in shortest paths and hence in a minimum quantity of material. It is also the most stable position since it corresponds to the minimum potential energy configuration: the net will return to this position in the event of slight perturbations. A cable net with a uniform tension along the geodesic lines is usually named “geotensoid”.
Most of the methods, available in the open literature, generate a “quasi” geotensoid cable net by projecting a plane pattern on the parabolic surface [3], sometimes approximated by a spherical surface. Then, they improve the accuracy by changing the node positions with iterative approaches or optimization algorithms. One method has been for example proposed by Tibert [6], however resulting in a variation of tensions in the cable elements (this technique will be more deeply discussed in section 2.3). In all cases, since these approaches can not guarantee a

uniform tension in the net, they do not produce the true minimal length configuration of the tension truss.
In this paper, we propose therefore an innovative method to generate cable nets with a uniform tension and forming exactly a parabolic surface. First, we present the approach, based on the force density method, and the used mechanical considerations. Several applications are then shown to illustrate the efficiency of method.
Space antennas also require a very low shape error for their parabolic surface. Faceting is generally the second main source of surface error after manufacturing, even if it is also due to thermal distortion, mesh saddling and deployment repeatability. We therefore present some considerations on the accuracy of computed surfaces by estimating the root mean square (rms) faceting error. Finally, problems about connecting the tension truss to a rim structure are discussed.

2. Geotensoid tension truss form-finding

2.1 Cable net form-finding with Force Density Method

The Force Density Method (FDM) was developed by Linkwitz and Schek [7], mainly to design the roof of the Munich Olympic Stadium in 1972 based on a tensile cable net covered with Plexiglas panels (Figure 3a). Calculation of both geometry (node positioning) and tension distribution was firstly based on physical models, measured with photogrammetry and extrapolated at scale one, but unsuccessful results have lead to the proposal of a new numerical approach.

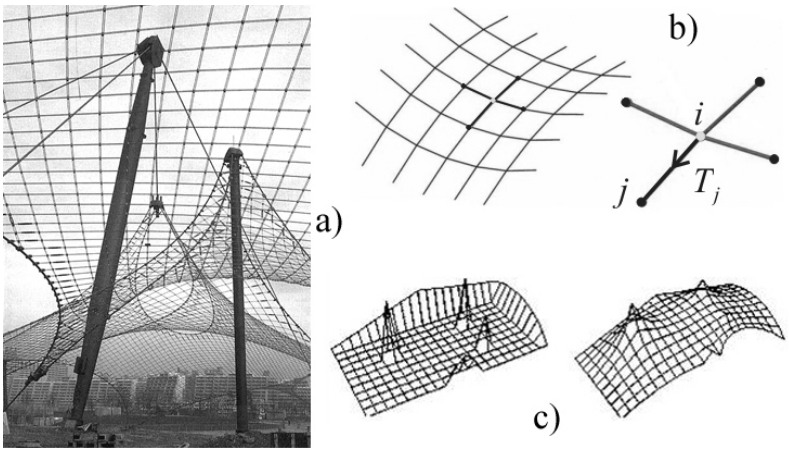

Figure 3: a) Munich Olympic Stadium roof; b) cable net equilibrium; c) Force Density Method

The principle of FDM is to linearize the equilibrium equations of the nodes connecting the tensile cable elements. We isolate a node *i*, connected to c_i cables of length ℓ_j with tension T_j and without external forces (Figure 3b). The node equilibrium, written on $\vec{X}$ direction of a coordinate system $(\vec{X},\vec{Y},\vec{Z})$ [1], implies that:

$$\sum_{j=1}^{c_i} T_j (X_j - X_i)/\ell_j = 0 \qquad (1)$$

[1] See nomenclature at the end of paper

The same relations may be written in $\vec{Y}$ and $\vec{Z}$ directions. However, these non linear equations can be linearized by introducing a "force density" coefficient q_j for every cable element (equal to the ratio of its tension by its length). This results in the following "barycenter" writing:

$$\sum_{j=1}^{c_i} q_j (X_j - X_i) = 0 \text{ and thus } X_i = (\sum_{j=1}^{c_i} q_j X_j) / (\sum_{j=1}^{c_i} q_j) \qquad (2)$$

Applying this approach to the whole network leads to a "node to node" process where successive nodal positions are computed until the global equilibrium is obtained. Cable tensions are then evaluated by $T_j = q_j \ell_j$. The FDM is implemented in numerous form-finding software (mainly in textile architecture): the designer generates an initial flat net and specifies anchoring conditions (Figure 3c). The resulting equilibrated shape depends on the set of force density coefficients. This method was then improved to investigate minimal configurations, mainly uniformly tensioned nets [8]. It is known that such net is also of minimal length. To perform such calculation, an iterative strategy can be used. The principle is to iterate on the force density coefficients to eventually obtain a required uniform tension T_u. For instance, if step *p* gives tension T_j^p in an element *j*, then the new coefficient used in the following step is:

$$q_j^{p+1} = q_j^p T_u / T_j^p \qquad (3)$$

If the boundary conditions allow forming a uniformly tensioned cable net, this method generally converges to a solution. However, conditions for convergence have not been explicitly written. This analysis is indeed difficult to achieve since it depends on many factors such as the net topology and the anchoring conditions.

An application is presented in Figure 4 where an anticlastic saddle shape (not an antenna) is computed with identical force density coefficients (a) and, then, with different coefficients to obtain a uniform tension (b). The difference in terms of resulting shapes may be clearly observed.

In the first case (identical coefficients), it has been demonstrated [9] that the computed net minimizes the sum of the squared element lengths $\sum \ell_j^2$. We insist on this point because a common mistake is to think that it minimizes the sum of the lengths $\sum \ell_j$.

In the second situation, the cable elements have the same tension, thus following the geodesic lines of the surface they describe. It also implies that only this configuration minimizes the sum of the lengths. However, it may be observed in this saddle shape application that the geometry is less regular than the previous one.

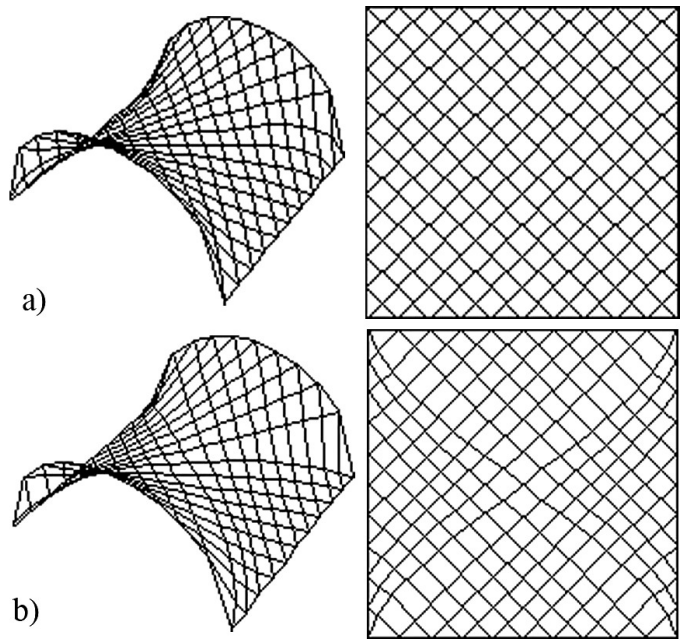

Figure 4: Saddle shape with a) identical force density coefficients; b) uniform tension

Nevertheless, we observe that the method generates only anticlastic surfaces. To obtain equilibrated synclastic surfaces, additional external forces must be applied at every node.

2.2 Parabolic reflective surfaces

The tension truss concept considered for the antenna in this paper is based on two cable nets: a "front" one (associated to the reflective surface) connected by tension ties to a mirrored "rear" one with the same shape (Figure 5). The ties allow forming synclastic shapes by ensuring the tension equilibrium in both nets (playing the role of "external" forces).

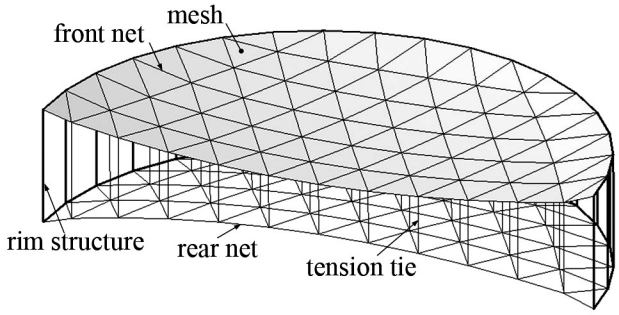

Figure 5: Front cable net (with the reflective mesh) and rear net with tension ties

Parabolic antennas are based on the same principle: all incident rays parallel to the paraboloid axis converge to the focal point (feed) after reflection on the surface. Conversely, all emitted rays are reflected parallel to the paraboloid axis. The reflector surface is defined by the intersection of a "parent" revolution paraboloid (with diameter D_p) and a cylinder (diameter D_a) parallel to the paraboloid axis which characterizes the antenna aperture.

In "prime focus" antenna (Figure 6), the axis of parent paraboloid and cylinder are coincident. The reflector surface is thus a paraboloid of revolution ($D_p = D_a$). In a Cartesian coordinate

system $(\vec{X},\vec{Y},\vec{Z})$, $\vec{Z}$ being the axis of revolution, the equation describing this axi-symmetric parabolic surface is:

$Z = (X^2 + Y^2)/(4F)$ where F is the focal length (4)

The height H_a of a reflector with diameter D_a is thus $H_a = D_a^2/(16F)$.

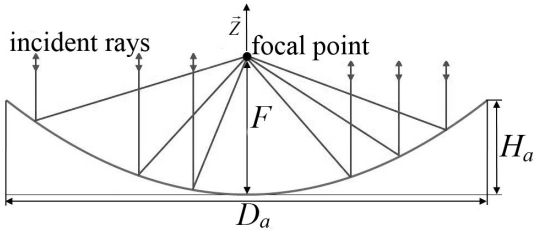

Figure 6: Prime focus parabolic reflector

One drawback of the axi-symmetric reflector is that the feed and its support are bulky and can block a part of the rays. To eliminate this problem and improve performance, antennas with offset feed are used. The cylinder axis is therefore separated to the paraboloid revolution axis of an offset distance d and $D_p = d + D_a/2$ (Figure 7).

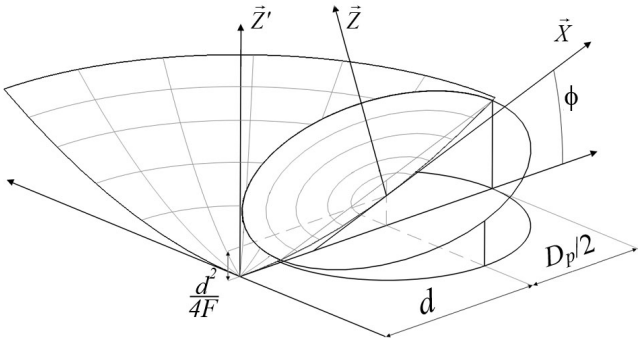

Figure 7: Axonometric view of offset parabolic surface

In the coordinate system $(\vec{X},\vec{Y},\vec{Z})$ (with an angle ϕ between $\vec{X}$ axis and the plane perpendicular to the paraboloid axis), the equation of the surface is in the form of $Z = f(X,Y)$:

$$Z = (a - \sqrt{b})/\sin^2\phi \quad \text{with} \quad \begin{cases} a = 2F\cos\phi + \sin\phi(d + \cos\phi\, X) \\ b = 4F\sin\phi\, X - \sin^2\phi\, Y^2 + (2F\sin\phi + \cos\phi\, d)^2 \\ \tan\phi = d/(2F) \end{cases} \quad (5)$$

This surface is symmetric in relation to $(\vec{X},\vec{Z})$ and its peripheral points are located on an flat ellipse parallel to $(\vec{X},\vec{Y})$.

2.3 Form-finding strategy

To calculate a geotensoid cable net forming a parabolic surface, the proposed method is to act on the additional forces due to the tension ties (on $\vec{Z}$ direction) connecting the front and rear cable nets. Their value will be chosen to ensure the node positioning on the surface defined by the relationships in Eq. 4 or 5.

From an initial net and a given set of force density coefficients q_j, the equilibrium position of a node *i* on $\vec{X}$ and $\vec{Y}$ directions is determined by the FDM (Eq. 2). With these two coordinates and the surface equation, the corresponding accurate position along $\vec{Z}$ is determined. The force in the tension tie necessary to equilibrate the node along this direction is then calculated by:

$$F_{Z_i} = \sum_{j=1}^{c_i} q_j (Z_j - Z_i) \qquad (6)$$

Lengths and tensions in the cable elements are next calculated and the condition of uniform tension is tested. The process is resumed by iteratively changing the force density coefficients (Eq. 3) until it results in the same tension T_u in every cable connected to node *i*. This method is successively applied to all the free nodes until (i) a uniform tension is obtained in all the cables, (ii) the nodes are in equilibrium and (iii) their positions do not vary.
If the process converges, a uniformly tensioned synclastic cable net with every node exactly on the parabolic surface is computed. The overall method is presented in Figure 8 as an algorithm.

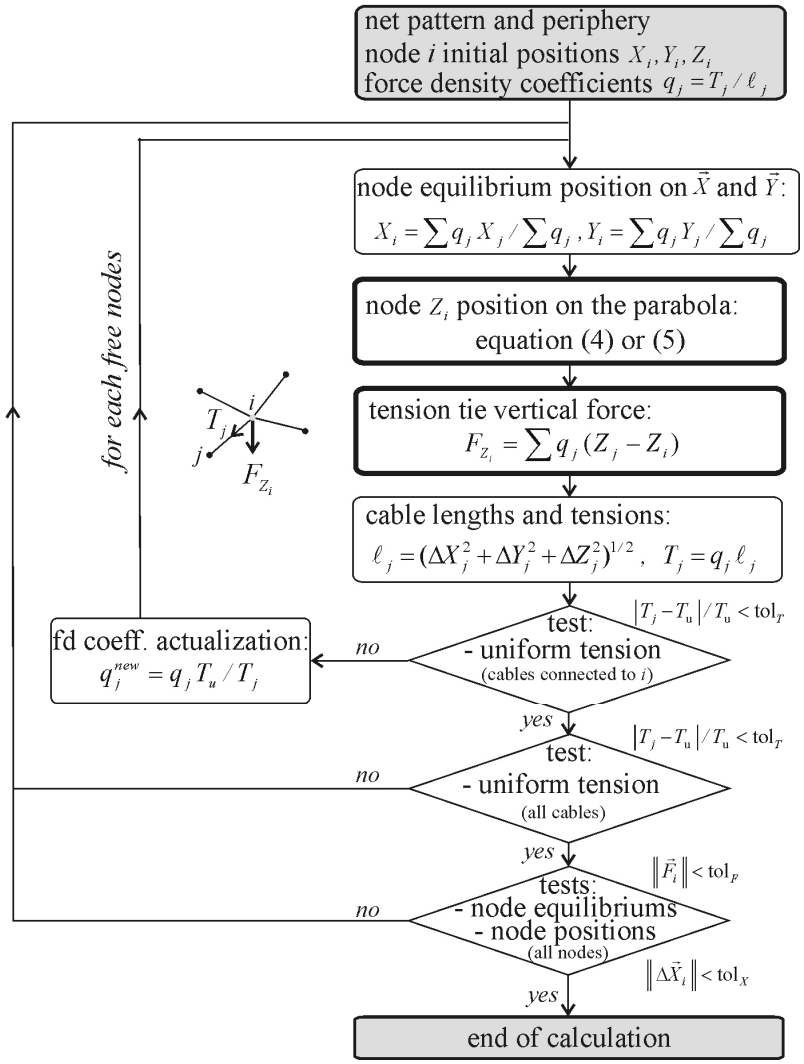

Figure 8: Algorithm for geometry calculation

The criterions used to decide on convergence are the following. To check the uniform tension requirement, it is verify if the difference with the objective T_u is lower than a tolerance tol_T (set to 0.1% in the applications presented in the next section). Moreover, a node is considered in equilibrium if the norm of its total out-balanced force $\vec{F}_i$ is inferior than tol_F (10^{-5} N in applications) and considered stable in position if between two consecutive iterations, its coordinates variation $\Delta\vec{X}_i$ is inferior than tol_X (set to 10^{-6} m).

Compared to the method proposed by Tibert in [6], this approach guarantees a uniform tension and a node positioning exactly on the parabolic surface (that is to say the computation of a true geotensoid configuration). In [6], a starting plane net with identical force density coefficients is first vertically projected on the surface. We note that these two configurations can not have a uniform tension and a minimal length. Then, forces in the ties are calculated to ensure the vertical equilibrium for each node by assuming a constant tension in the cable elements. These forces are subsequently homogenized by rounding their values to integers (multiples of 1 N, to reduce the spectrum of values). The net corresponding to that distribution is then computed while keeping the nodes on the parabolic surface. Nevertheless, in the application presented for a 12.25 m offset antenna, tensions in the cables vary from 41 N to 120 N, hence meaning a non constant distribution and a non geotensoid truss.

2.4 Applications on tension trusses

2.4.1 Prime focus configuration

The method has been applied on several types of cable nets. The initial net patterns are planar and located inside a circle which represents the antenna anchoring structure. The rim nodes are located on a circle (center at $X = 0$ and $Y = 0$, diameter D_a).

Figure 9a shows an example of a 6 by 6 “diamatic” pattern, one of the most frequently used. It is composed of 6 disc sectors where each boundary side is divided into 6 elements. The resulting net, forming an axi-symmetric paraboloid with a uniform tension, is presented in Figure 9b. This pattern is based on triangular facets but the triangles are definitively not equilateral and identical (elements with different lengths, as for a geodesic dome). It is clear that no geotensoid configuration for a paraboloid using equilateral triangles exists.

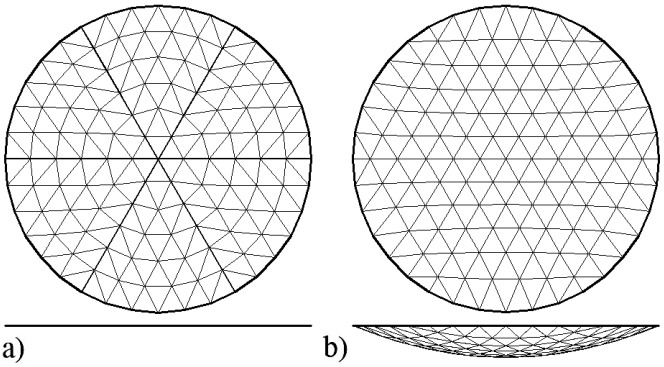

Figure 9: Diamatic net on axi-symmetric paraboloid: a) initial flat net; b) computed net

Figure 10 shows the distribution of forces in the tension ties for $D_a = 12$ m and a specified net tension equal to 100 N in every cable element. In case of F / D_a respectively equal to 0.4 and 0.6, the average tie force is 32.17 N and 22.36 N (with standard deviations 2.60 N and 0.89 N).

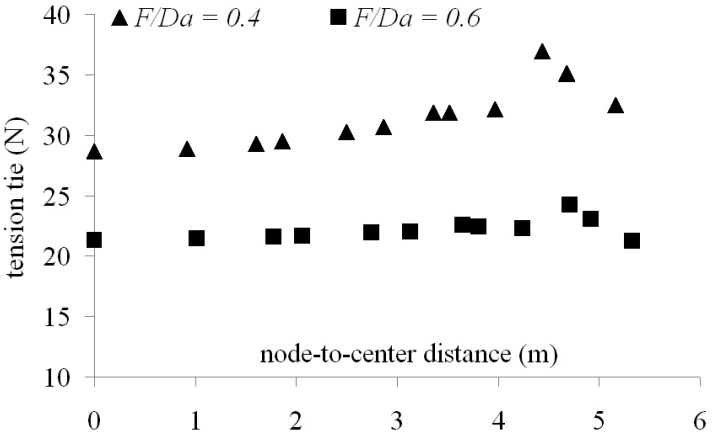

Figure 10: Tension tie force distribution in axi-symmetric case

The computation method has been tested on different patterns and some computed nets are presented in Figure 11. The method eventually converges but the resulting nets are highly dependent on the pattern and, in some cases, the facet size can vary widely.

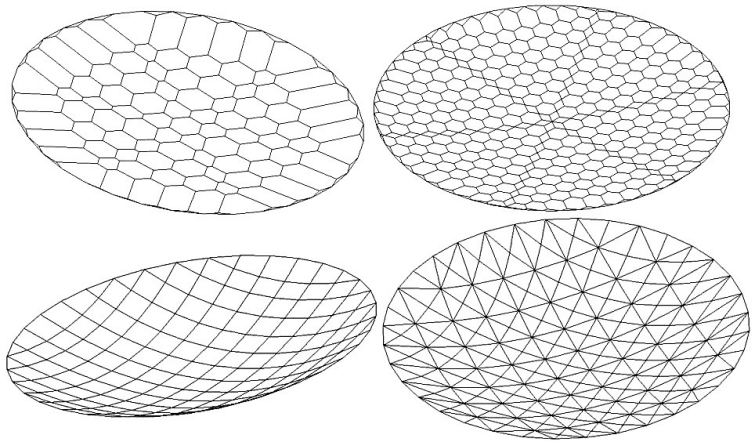
Figure 11: Different calculated configurations

2.4.2 Convergence

The conditions for convergence of the algorithm are difficult to write analytically. We however present in Figure 12 some graphs showing the variation of the position for two nodes during iterations: one is at the center of the axi-symmetric paraboloid ($D_a = 12$ m, $F / D_a = 0.6$); the other one is located laterally and close to the peripheral rim circle. In this case, computations converge to stabilized equilibrium positions after 200 iterations.

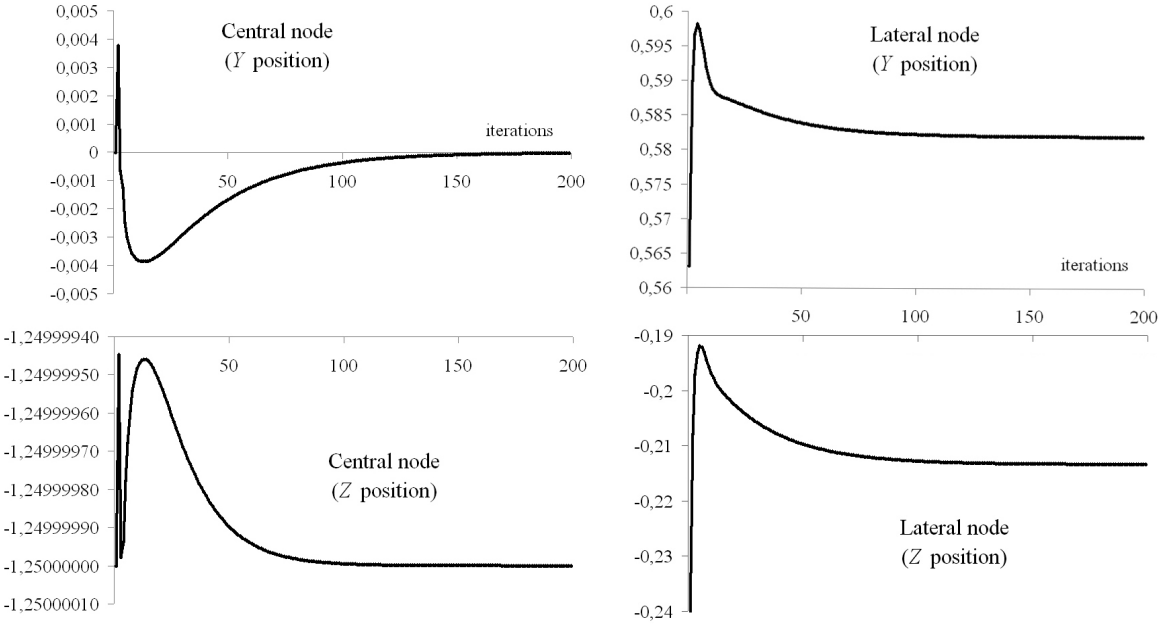

Figure 12: Two nodes positioning during iterations (values of coordinates *Y* and *Z* in m)

2.4.3 Offset configuration

The three main parameters of offset reflector are the aperture diameter D_a, the focal length F and the offset distance *d*. A large diameter results in a higher gain. The focal length (or the F / D_p ratio) must not be too high for structural reasons. The offset distance should be large enough to eliminate the obstruction of rays by the feed.

Hence, the first numerical application is given for $D_a = 12\,\mathrm{m}$, $F / D_p = 0.45$ and $d = 8.3\,\mathrm{m}$ (values close to those of existing reflectors like AstroMesh [10], Figure 2b). A diamatic pattern of 6 sectors of 10 divisions is considered with peripheral nodes attached to an elliptical rim structure (center at $X = H_a \sin\phi$ and $Y = 0$) at the altitude $Z = H_a \cos\phi = H_o$. The transverse diameter of the rim structure is $D_a/\cos\phi$ (on $\vec{X}$) and its small diameter is equal to D_a (on $\vec{Y}$).

For a 100 N uniform tension in the net, the form-finding method converges to an average force in the tension ties close to 7.14 N (standard deviation 0.53 N). The resulting force distribution is presented in Figure 13.

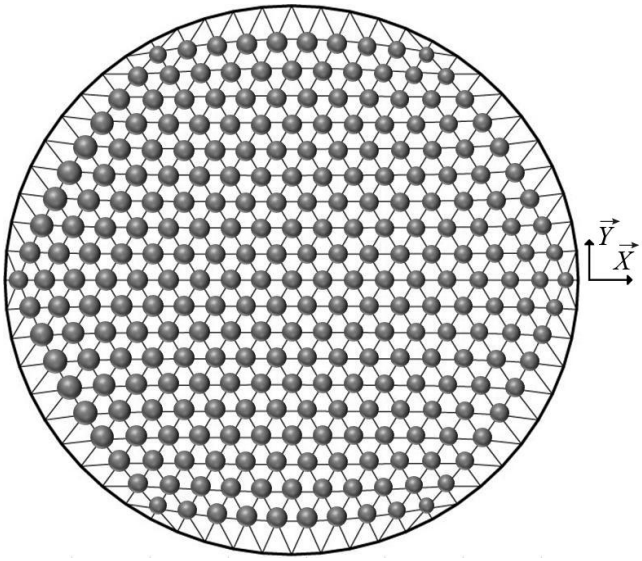

Figure 13: Tension tie force distribution in offset case with elliptical rim (sphere diameter proportional to the tension tie force)

A second application is given to illustrate the case where the net is connected to edge tensile cables (such as for the Halca reflector, Figure 2a). We consider the same antenna characteristics ($D_a = 12\,\mathrm{m}$, $F / D_p = 0.45$, $d = 8.3\,\mathrm{m}$, 100 N uniform tension) and the resulting net is presented in Figure 14. Tension tie forces in the net vary from 11.68 N to 6.69 N (average force 10.38 N, standard deviation 0.84 N). Higher forces (ranging from 22.67 N to 60.26 N) appear for the nodes connected to the edge cables. The force density coefficients for these edge elements have been set constants; it results in a maximal tension of 1154 N and the corresponding peripheral nodes are not on the parabola.

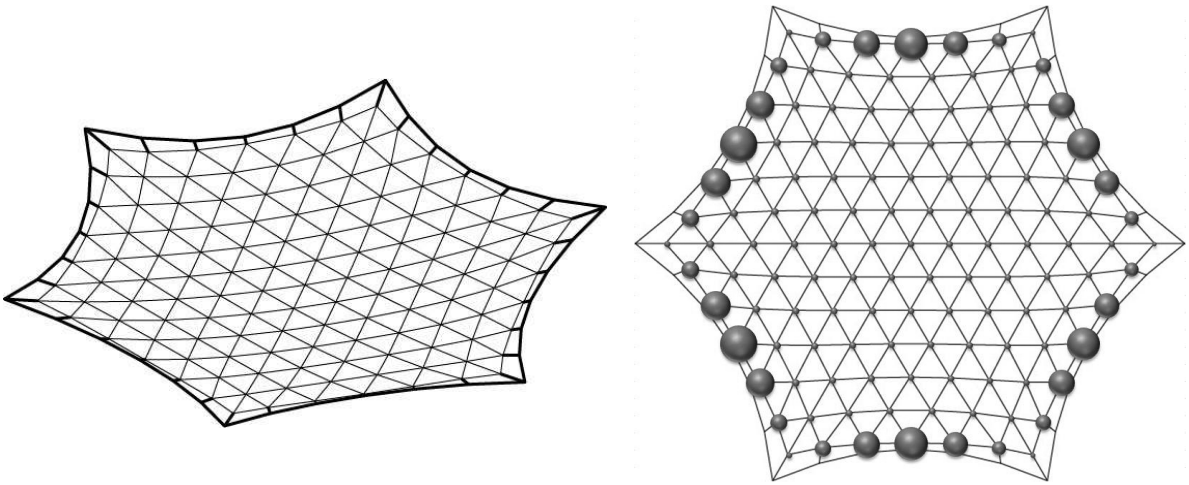

Figure 14: Offset antenna with edge cables (isometric view and top view with tension tie force distribution given by spheres)

Since the main driving parameter is the “quality” of the obtained surface, we have now to discuss if the computed nets by the proposed form-finding method give an acceptable surface error due to faceting.

3. Systematic faceting error

The ideal mathematical shape defined by eq. (4) or (5) is however purely theoretical since it has to be realized by a faceted mesh stretched on the tension truss. The typology of the net determines the forms and dimensions of the flat facets. The faceted (and discrete) surface no longer corresponds to the continuous one. The parabolic surface that the faceted paraboloid best approximates may be then calculated; this is referred to as the "best-fit paraboloid" (Figure 15). It is characterized by a resulting focal length variation and a translation compared to the theoretical surface.

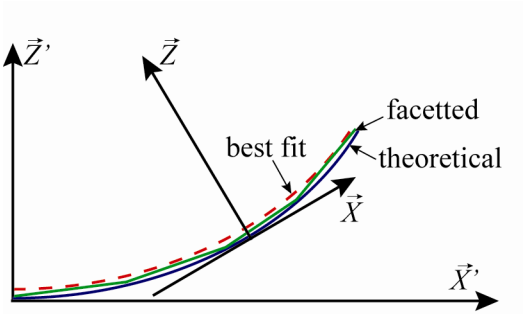

Figure 15: Best fit paraboloid

The faceting error is limited relatively to the shortest wavelength to be transmitted. For example, in the 12 m AstroMesh reflector, the faceting rms error is 1.15 mm [11].
Different approaches have been proposed to calculate this error. Agrawal [12] estimates that, if the reflector is shallow, it can be approximated by a sphere of radius $2F$. In this case, the faceting rms error with regular polygonal facets is close to $\delta_{rms} \approx L^2/(F\,C^2)$, where L is the facet length side and C a constant respectively equal to 7.872, 6.160 or 4.046 for triangular, square and hexagonal facets. This formula is often used to determine the maximum length of a net for a given error. In the case of $F = 12.87$ m (value considered for the offset paraboloid in section 2.4.3) and a faceting error of 1 mm, the length of triangular facet side calculated with Agrawal's relation should be less than 0.893 m. In the 6 by 10 diamatic net with an elliptical rim that we have computed (Figure 13), the maximal cable length is 0.898 m while the average length is 0.685 m (which corresponds to an error of 0.59 mm with Agrawal's relation).
Because of such difference, we tried to estimate the faceting error in order to take into account the irregularity of facets. To do this, techniques like the half-path length method [13] are available to compute the surface error due to imperfections by comparing pairs of points (the first one on the real paraboloid, the second one on the theoretical paraboloid). Results however depend on the number and on the type of chosen points. Since our study only aims to estimate the error, we decided to compare only the Z'_{g_t} values (position of the gravity centre of every computed triangular facets t on the vertical axis $\vec{Z}'$ of the parent paraboloid) with the Z'_t values (theoretical position of this point on the parabolic surface calculated with the (X'_{g_t}, Y'_{g_t}) coordinates). The "axial" faceting rms error is in this case given by [2]:

$$\delta_{rms} = (\sum_{t=1}^{n} A_t (Z'_t - Z'_{g_t})^2 / \sum_{t=1}^{n} A_t)^{1/2} \qquad (7)$$

where A_t is the projected area of the triangular facet on the plane $(\vec{X}', \vec{Y}')$. The best fit paraboloid which minimizes the faceting rms error is the theoretical paraboloid transformed with a translation $\Delta Z'$ along $\vec{Z}'$ direction and two rotations around $\vec{X}'$ and $\vec{Y}'$ axis. However, these rotations are small and assumed to be negligible in the application we will present. To improve again the accuracy, the focal length F_{bf} of the best fit paraboloid may be also adjusted.
The resulting equation of the best fit paraboloid is:

$$Z'_{\text{bf}} = (X'^2 + Y'^2)/(4F_{\text{bf}}) + \Delta Z' \qquad (8)$$

For the configuration we study (diamatic net with elliptical rim), the axial faceting rms error obtained by (7) is roughly 3 mm. The error relative to the best fit paraboloid (where Z'_{bf_t} replace Z'_t in (7)) is 0.33 mm. The large difference between the two errors can be explained by the fact that the best fit paraboloid is closer to the centers of gravity of the triangles and no longer to the cable intersections (as for the initial theoretical paraboloid). The translation $\Delta Z'$ is quasi equal to this difference and can be determined by the following relation:

$$\Delta Z' = \sum_{t=1}^{n} A_t (Z'_t - Z'_{g_t}) / \sum_{t=1}^{n} A_t \qquad (9)$$

The parameter $\Delta Z'$ and F_{bf} of the best fit paraboloid can be determined by standard optimization algorithms to reduce the error, like Newton's or conjugate gradient methods (we used the Excel™ solver in this study).

3.1 Results

Several computed diamatic nets in offset configurations are presented in Table 1 to compare the incidence of the discretization (number of facets) and of the F / D_p ratio. It shows that the faceting error increases if the number of facets is reduced or if the curvature is larger. We also observe that the presented computation method provides a faceting error lower than 1 mm, even with few facets.

Number of divisions	5	6	8	10	10	10
Number of triangular facets *n*	150	216	384	600	600	600
Ratio F / D_p	0.45	0.45	0.45	0.45	0.30	0.60
Faceting error δ_{rms} (mm)	*12.19*	*8.50*	*4.80*	*3.08*	*5.04*	*2.24*
Error with only $\Delta Z'$ translation (mm)	*1.05*	*0.79*	*0.49*	*0.34*	*0.88*	*0.21*
Error with $\Delta Z'$ & F_{bf} optimization (mm)	*0.99*	*0.75*	*0.48*	*0.33*	*0.82*	*0.21*

Table 1: Faceting errors for diamatic nets with all the nodes on the parabolic surface

3.2 Connection to the rim structure

The attachment of the net to the antenna rim implies boundary conditions which are not necessarily compatible with all net patterns. For example, in case of the AstroMesh, the rim is

realized with a 30 bays ring. The net is thus attached at 30 points to the ring truss, whereas it requires 60 points to fix a 6 by 10 diamatic pattern.

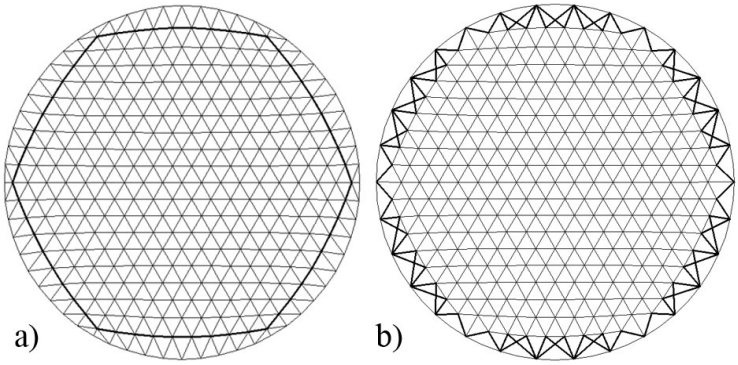

Figure 16: Diamatic net a) under uniform tension; b) like the Astromesh net

For this specific pattern, the method can be the following. We firstly performed the form-finding with all nodes on the paraboloid (with elliptical rim). Then we extract a 6 side's part with 9 elements on each side to create the reflective zone (Figure 16a). This "hexagonal" net is connected to the rim by a new set of anchoring cables. Each side node is attached to the rim by two cables for which the tensions are calculated to keep a uniform tension in and on the hexagon. Figure 16b shows a pattern like the AstroMesh net but other configurations are possible [3] while there are at least two cables to ensure the equilibrium of nodes. The tensions in these two elements are calculated to equilibrate the resulting force due to other connected cables in $\vec{X}$ and $\vec{Y}$ directions. The corresponding tension tie force is then revaluated to equilibrate the node in $\vec{Z}$ direction. This approach allows attaching a cable net to the rim structure without changing significantly the reflective surface and its accuracy. Only cables connected to the rim are not in the same tension T_u as the others. For T_u = 100 N, tensions in anchoring cables vary from 37 to 181 N. The resulting forces in tension ties are represented in Figure 17 for both configurations; they differ only close to the peripheral zone (between 5 and 6 m).

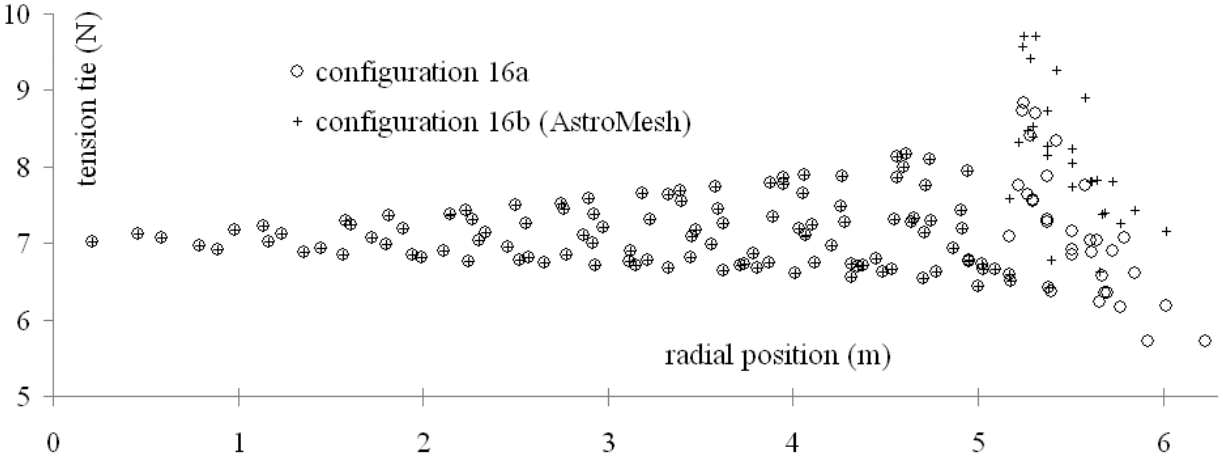

Figure 17: Tension tie force distribution with net to rim attachment

However, the kinematic and static indeterminacy must also be checked. This may be performed by determining the number of mechanisms *m* and of self-stress states *s* (with $m - s = C - 3(N - N_a)$ where *C*, *N* and N_a are respectively the number of cable elements, of nodes and of nodes attached to the rim) [6]. For such a big structure, it has to be calculated by computing the rank r_E of the equilibrium matrix $[E]$ of the structure (that verifies the global relationship $[E]\{q\} = \{0\}$ where the two nets with their tension ties are considered) and then using $m = b - r_E$.

For the configuration in Figure 16a with $C = 2191$, $N = 662$ and $N_a = 120$, it comes $r_E = 1626$ and therefore $m = 0$ (*i.e.* no mechanism) with $s = 565$ (self-stress vectors comprising tensile and compressive forces). For the configuration 16b (AstroMesh like) with $C = 2005$, $N = 590$ and $N_a = 60$, then $r_E = 1595$ and $m = 0$ with $s = 415$.

The results show that the tensioned net can be fitted to the rim without mechanism, even if the number of anchoring points is reduced.

4. Conclusion

A new method to calculate a uniformly tensioned cable net is presented. The approach is based on an improvement of the force density method: the idea is to use the nodal forces due to the tension ties to position them on the target surface. In an iterative computation, a cable net with a uniform tension is obtained by variation of the force density coefficients. Tests on different surfaces show the efficiency of the method. The obtained values of systematic faceting error show that this approach is able to meet the requirements of space applications. The proposed form-finding method hence provides nets with a low faceting error and a uniform tension, so a good reflectivity of the surface. It is applied for reflectors but could be used in other fields or applications to design uniformly tensioned synclastic surfaces.

Acknowledgments:
The “Laboratoire de Mécanique et Génie Civil” would like to thank the “Centre National d’Etudes Spatiales” (CNES) for its support in this work.

References

[1] K. Miura, Y. Miyazaki, Concept of the tension truss antenna, AIAA Journal, 28 (1990) 1098-104.
[2] A.G. Tibert, Deployable tensegrity structures for space applications, Ph.D. Dissertation, Department of Mechanics, Royal Institute of Technology, Sweden, 2002.
[3] A.G. Tibert, Optimal design of tension truss antennas, AIAA 2003-1629, 44th AIAA/ASME/ASCE/AHS/ASC Structures, Structural Dynamics and Materials Conference; Norfolk VA, 2003.
[4] J.M. Hedgepeth, M.W. Thomson, D. Chae, Design of large lightweight precise mesh reflector structures, Astro Aerospace Corporation Technical Document, AAC-TN-1164, 1991.
[5] V. Lubrano, R. Mizzoni, F. Silvestrucci, D. Raboso, PIM characteristics of large deployable reflector antenna mesh, MULTICOPIM 2003, ESA/ESTEC, 2003.
[6] A. Eriksson, A.G. Tibert, Redundant and force-differentiated systems in engineering and nature, Computer Methods in Applied Mechanics and Engineering, 195(41-43) (2006) 5437-53.
[7] K. Linkwitz, H.J. Schek, Einige Bemerkungen von vorgespannten Seilnetzkonstruktionen, Ingenieur-Archiv 40 Springer-Verlag (1971) 145-58.
[8] B. Maurin, R. Motro, Investigation of minimal forms with density methods, Journal of the International Association for Shell and spatial Structures, 38(3) (1997) 143-54.
[9] H.J. Schek, The force density method for form finding and computation of general networks, Computer Methods in Applied Mechanics and Engineering, 3 (1974) 115-34.
[10] AstroMesh™ deployable reflector data sheet, DS-409 07/04, Astro Aerospace, Northrop Grumman Space Technology, 2004.
[11] M.W. Thomson, Astromesh deployable reflectors for Ku- and Ka-band commercial satellites, 20th AIAA International Communication Satellite Systems Conference and Exhibit, Montreal, AIAA (2002) 2002-32.
[12] P.K. Agrawal, M.S. Anderson, M.F. Card, Preliminary design of large reflectors with flat facets, IEEE Transactions on Antennas and Propagation AP-29(4) (1981) 688-94.
[13] S.M. Barondess, S. Utku, Computation of weighted root-mean-square of path length changes caused by the deformations and imperfections of rotational paraboloidal antennas, Jet Propulsion Laboratory, Pasadena CA, Technical Memorandum (1963) 33-118.

Appendix A: nomenclature

A_t	projected area of mesh elementary triangle *t*
c_i	number of cable elements connected to node *i*
C	total number of cable elements
d	offset distance
D_a	aperture diameter
D_p	diameter of parent paraboloid
$[E]$	equilibrium matrix
δ_{rms}	root mean square error
ΔZ	axial translation
F	focal length
F_{bf}	focal length of the best fit paraboloid
F_{Z_i}	force in the tension tie connected to node *i*
H_a	height of axi-symmetric reflector
H_o	height of offset reflector
ℓ_j	length of cable element *j*
m	number of mechanisms
n	number of triangular facets in the mesh
N	total number of nodes
ϕ	angle between $\vec{X}$ and horizontal plane
q_j	force density coefficient for cable element *j*
s	number of self-stress states
T_j	tension in cable element *j*
T_u	uniform tension in the cable net
$(\vec{X},\vec{Y},\vec{Z})$	paraboloid coordinate system
$(\vec{X}',\vec{Y}',\vec{Z}')$	parent paraboloid coordinate system (case of offset reflector)